d-band hole dynamics in gold nanoparticles measured with time-resolved emission upconversion microscopy

Stephen A. Lee,[1,2‡] *Christopher T. Kuhs,*[3‡] *Emily K. Searles,*[1,2] *Henry O. Everitt,*[3,4] *Christy F. Landes,*[1,2,4,5,6] *Stephan Link**[,1,2,4,5]

[1]Department of Chemistry, Rice University, Houston, Texas 77005, United States

[2]Center for Adapting Flaws into Features, Rice University, Houston, Texas 77005, United States

[3]U.S. Army DEVCOM Army Research Laboratory-South, Houston, TX 77005

[4]Department of Electrical and Computer Engineering, Rice University, Houston, Texas 77005, United States

[5]Smalley-Curl Institute, Rice University, Houston, Texas 77005, United States

[6]Department of Chemical and Biomolecular Engineering, Rice University, Houston, Texas 77005, United States

‡Equal contribution

*To whom correspondence should be addressed: slink@rice.edu

KEYWORDS: Photoluminescence, plasmon, ultrafast, hot holes, interband transitions

Abstract

The performance of photocatalysts and photovoltaic devices can be enhanced by energetic charge carriers produced from plasmon decay, and the lifetime of these energetic carriers greatly affects overall efficiencies. Although hot electron lifetimes in plasmonic gold nanoparticles have been investigated, hot hole lifetimes have not been as thoroughly studied in plasmonic systems. Here, we demonstrate time-resolved emission upconversion microscopy and use it to resolve the lifetime and energy-dependent cooling of *d*-band holes formed in gold nanoparticles by plasmon excitation, and follow their decay into interband and then intraband electron-hole pairs.

Main

Over the past few decades, metal nanoparticles are increasingly used as hot carrier generators,[1–6] sensors,[7–9] and resonators.[10–12] Photoexcited hot carriers created through plasmon decay are able to drive photocatalytic and photovoltaic processes.[5,13–18] The lifetimes and energy distributions of these hot electrons are extensively studied.[3,6,19,20] Hot holes are also produced in plasmonic nanoparticles, especially by interband excitation,[21–24] and drive oxidation reactions,[25–28] despite their predicted short lifetimes.[21,29]

While hot electron lifetimes were investigated through transient pump-probe spectroscopy[6,30,31] and time-resolved two-photon photoemission spectroscopy (2PPS),[32–34] measuring hot hole lifetimes historically require less direct techniques. 2PPS demonstrated delayed generation of hot electrons due to Auger decay of *d*-band holes on the order of 50–60 fs.[32,35] Additionally, hole lifetimes in noble metals were estimated by the linewidth of one-photon photoemission spectra[36,37] and interferometric time-resolved two-photon photoemission spectroscopy (ITR-2PPS).[38] The energy dependence from the linewidth analyses gave a Fermi liquid theory relationship for the hole lifetime $\tau_h = 105\ fs \cdot eV^2\ (E_i - E_F)^{-2}$, or ~30 fs for a hole with an energy below the Fermi energy of $E_i - E_F = 1.9$ eV.[36,37] Similarly, ITR-2PPS gives a hole lifetime of ~30 fs at 1.9 eV and 50 K and ~55 fs at 1.9 eV and 300 K in Cu, revealing a temperature dependent hole-phonon scattering dependence and an Auger scattering contribution of 24 fs.[38] A Fermi liquid theory dependence is not necessarily expected due in part to symmetry properties[36] and because Fermi liquid theory formally describes the interaction of a single excited electron within a sea of conduction band electrons.[39] *Ab initio* calculations showed that the energy dependence of the hole lifetime deviates from Fermi liquid theory, while the reported hole lifetimes vary significantly, 10–70 fs.[21,29,37,40] Given the interest in plasmon-induced hot carrier generation, there is a need to know the lifetime of the photoexcited holes produced in plasmonic nanoparticles under ambient and, in the future, photocatalytic conditions. To our knowledge, no direct measurements of *d*-band hole lifetimes in ligand free plasmonic gold nanoparticles have been performed.

Here, we report measurements of the energy-dependent lifetime of hot holes in gold nanoparticles and a thin gold film using time-resolved emission upconversion microscopy. We obtain <100 fs temporal resolution through optical gating by sum frequency mixing of the emission with an ultrashort gate pulse. The optical layout and spectral and temporal profiles of the gate and pump pulses are presented in Figures 1 and S1 and summarized in the Supporting Information. This time-resolved emission upconversion microscope has a gate autocorrelation full width at half maximum (FWHM) of 72 fs (Figure 1B) and a gate and pump cross-correlation of 96 fs FWHM (Figure 1C). The cross-correlation is used as the instrument response function (IRF). Deconvolution of these pulses results in a FWHM of ~50 fs and ~70 fs for the gate and pump pulses, respectively.

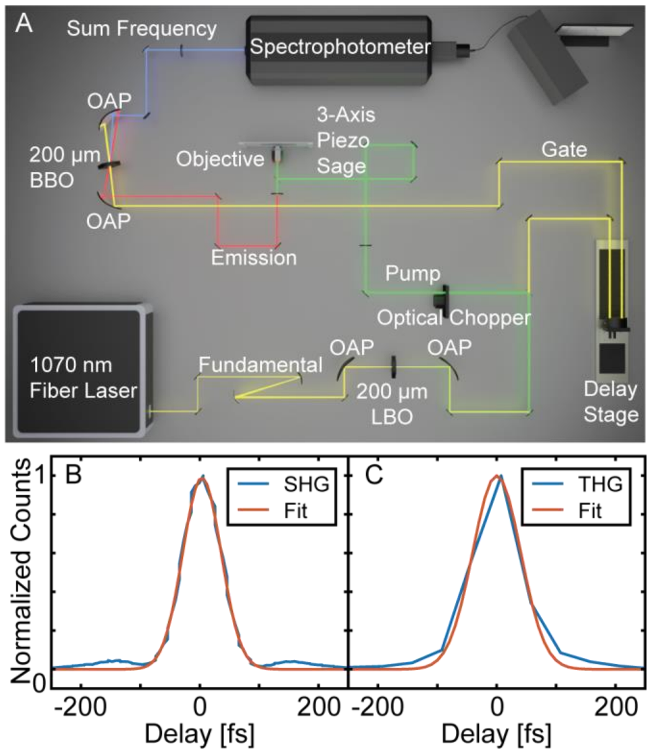

Figure 1. Time-resolved emission upconversion microscopy. (A) Layout of the microscope with important optics listed: Off-axis parabolic mirror (OAP), lithium triborate (LBO) crystal, beta-barium borate (BBO) crystal. (B) Auto-correlation of the fundamental pulse producing second harmonic generation (SHG, blue) and a $Sech^2$ fit to the data (red). (C) Cross-correlation of the fundamental and second harmonic pulses producing third harmonic generation (THG, blue) and a $Sech^2$ fit (red).

Additionally, our pump beam waist at the focus is ~2.6 μm (Figure S1), which represents a compromise with optimized temporal resolution using all reflective optics including the objective.

Light emission from gold films, when excited above the interband threshold, has previously been assigned to the radiative recombination of *sp*-band electrons with *d*-band holes.[41] This process is enhanced through the local electric fields of surface plasmons when nanoscale roughness is introduced.[42] Thus, the time-resolved interband emission from gold nanoparticles should directly report the lifetime of the *d*-band holes. We use our microscope to measure the time-resolved emission from a plasmonic gold nanoparticle substrate compared to a thin gold film when excited at 535±12 nm. The samples are fabricated by evaporating a 10 nm thin gold film onto two separate glass slides. The nanoparticles are formed by thermally annealing one of the gold films. Both the gold nanoparticles and film are overcoated with an inert 30 nm Al_2O_3 layer to increase sample stability.[43] This fabrication procedure (see the Supporting Information) is chosen to reduce sources of impurity emission from molecular adsorbates such as surface ligands, as well as to prevent photoexcited hot carriers from reacting at the interface, as Al_2O_3 prevents additional plasmon damping channels such as charge transfer.[44]

The gold nanoparticle absorbance spectrum exhibits a broad plasmon resonance, which is much weaker for the gold film (Figure 2A). Because of overlap with interband absorption, plasmon decay in our case mainly results in excitations from the *d*-band to above the Fermi energy.[45] Scanning electron microscopy reveals that the gold nanoparticles are roughly 120±50 nm in diameter with a coverage of ~50 particles per μm^2 (Figure 2A inset). This particle density and the observation area of our time-gated upconversion emission microscope mean that we are probing ~500 nanoparticles. The photoluminescence from 532 nm continuous wave excitation of the gold nanoparticles displays a broad peak centered at 590 nm (Figure 2B). This spectrum is consistent with one-photon excited photoluminescence due to radiative recombination of interband transitions, as reported for gold films and single gold nanoparticles.[41,46–48] When switching to 535±12 nm pulsed laser excitation, we still observe a one-photon emission process within our pump power range as confirmed by a linear pump power dependence of the integrated emission intensity (Figure 2C) and wavelength resolved power law of 1 for our spectral region of interest (Figure S3). A nonlinear component, as observed previously under pulsed excitation,[49–51] is present close to the pump wavelength, but is spectrally excluded in the time-resolved experiments. The photoluminescence for the gold film is weaker due to less plasmon enhancement than the nanoparticle sample (Figure 2B).[42] However, the film is thin enough that surface roughness likely plays a role and lends the sample weak plasmonic character.[52,53] This interpretation is further supported by comparing the emission intensity of the gold film to a thicker 30 nm gold film that has a 9 times lower intensity despite its larger volume (Figure S2).

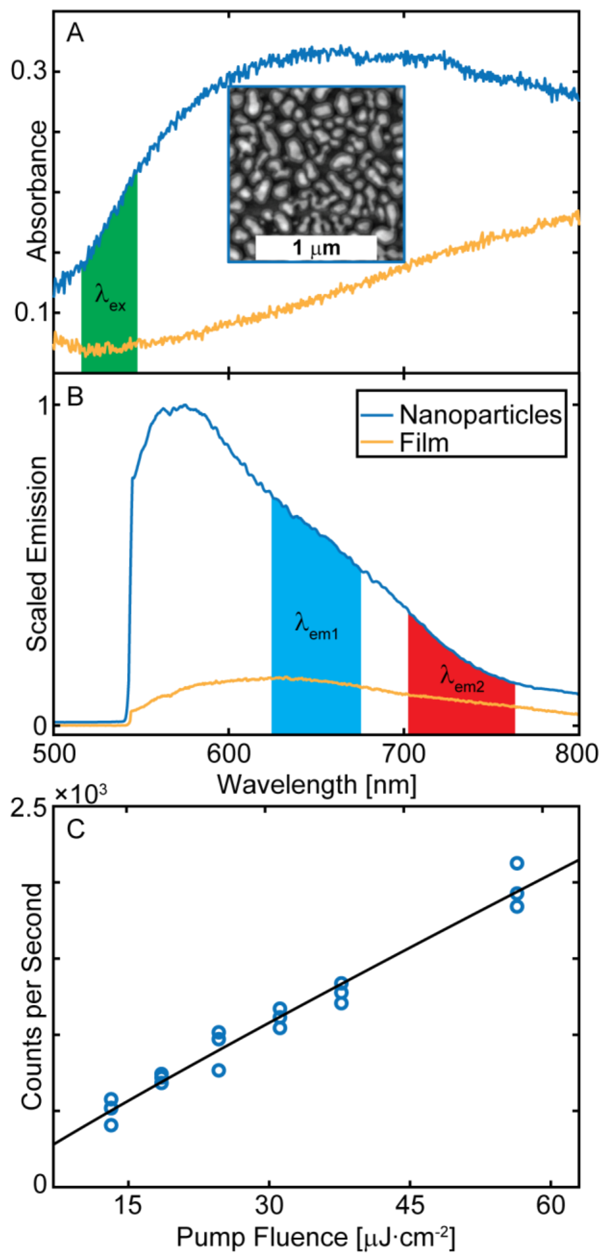

Figure 2. Characterization of the gold nanoparticles and the thin gold film. (A) Visible to near-infrared absorbance of the nanoparticles (blue) and film (gold). For the gold nanoparticles the plasmon is peaked at 650 nm. Inset: scanning electron micrograph of the gold nanoparticles. (B) Emission spectra of the nanoparticles (blue) and film (gold), excited with a 532 nm continuous wave laser. The shaded regions at 650±25 nm and 730±25 nm indicate the emission bands interrogated with time-resolved emission upconversion microscopy. (C) Excitation pump power dependence of the nanoparticle emission integrated over the entire spectrum, excited with 535±12 nm pulses. A power law fit (black line) gives an

exponent of ~1, confirming a one-photon emission process for our spectral region (see also Figure S3). The power dependence, performed three times in random order, illustrates the absence of photothermal damage to the sample. Additionally, good stability against photothermal damage is confirmed by comparing the emission spectra recorded before and after illumination with the highest pump power (Figure S3).

The time-resolved emission of the gold nanoparticles upon 535±12 nm (2.3 eV) pulsed excitation is illustrated in Figure 3A. The 1070 nm gate pulse is optically mixed at different pump-gate delay times with the emission from the sample using a BBO crystal that is tuned to maximize the sum frequency generation of 650 nm emission. We fit the measured gold nanoparticle emission time-traces and obtain an interband emission lifetime of τ_{em} = 57±5 fs (Figure 3A), where the error is from the 95% confidence interval of the fit.

We interpret this emission lifetime at 650±25 nm as the lifetime of hot holes formed in the *d*-band following plasmon decay into interband excitation of *d*-band electrons to empty electronic levels of the *sp*-band above the Fermi energy, as illustrated by the upward arrow in Figure 3B and 3C. These hot holes cool through a combination of energy-dependent radiative and non-radiative relaxation with characteristic rates k_r and k_{nr}. Given that the quantum yield (QY) is the ratio of the radiative rate to the total rate, $\mathrm{QY} = \frac{k_r}{k_r + k_{nr}}$, and for large gold nanoparticles QY ≈ 10^{-8},[54] it follows that $k_r \ll k_{nr}$, and thus the emission lifetime is dominated by k_{nr}. The measured hole lifetime, τ_h, revealed by the interband emission lifetime, is given then by $\frac{1}{\tau_{em}} = k_r + k_{nr} \approx k_{nr} = \frac{1}{\tau_h}$. We assume that τ_h is equivalent to τ_{em} given that interband emission occurs from an *sp*-band electron near the Fermi Energy recombining with the *d*-band hole, as illustrated by the downward arrow in Figure 3B.[41] We rule out contributions to τ_{em} from hot electron lifetimes since we are probing the Stokes shifted interband recombination, which involves *sp*-band electrons at or below the Fermi energy recombining with the d-band holes.[41,42,55] We can also estimate the radiative and nonradiative rates according to $k_r = \mathrm{QY}/\tau_{em}$, resulting in k_r and k_{nr} on the order of 170 ms^{-1} and 17 ps^{-1}, respectively, for τ_{em} = 57 fs and assuming a QY of 10^{-8}.

Nonradiative relaxation includes hole scattering within the d-band. The process that overall determines how long a hole excitation in the *d*-band survives is efficient Auger scattering where an *sp*-band electron fills the *d*-band hole providing the momentum and energy to promote a different *sp*-band electron to an empty state above the Fermi energy, thus converting a hot hole into a hot electron (Figure 3C dashed arrows).[32,35] Interestingly, τ_h is longer than extracted from previous studies (~30 fs, see red line in Figure 3A) that were not able to measure hole lifetimes directly.[36] τ_h is instead similar to the lifetimes of electrons generated by Auger scattering (50–60 fs),[32] consistent with our interpretation that the dominating nonradiative channel we observe is Auger scattering.

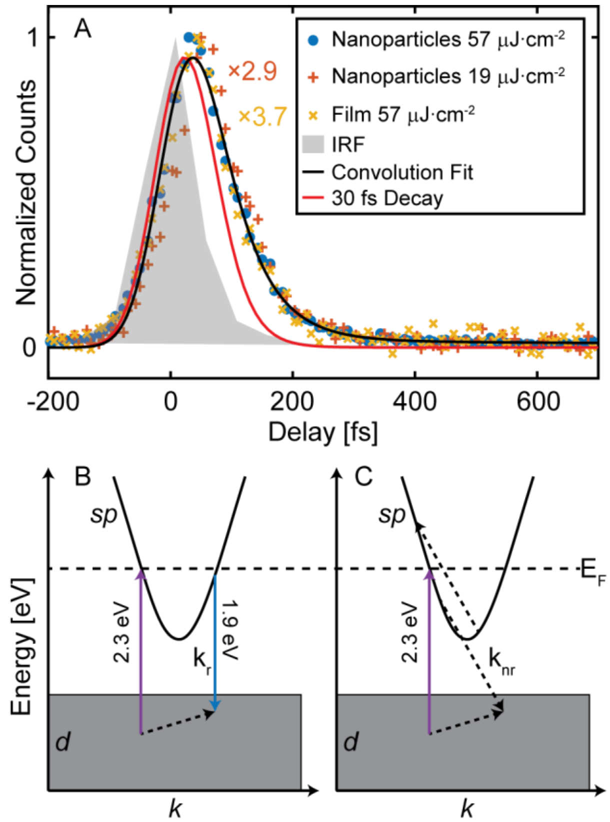

Figure 3. Time-resolved emission dynamics of gold nanoparticles and film. (A) Time-resolved emission of the gold nanoparticles and gold thin film measured at a center emission wavelength of 650 nm. A convolution fit of the data reveals an emission decay time of 57±5 fs, corresponding to the *d*-band hole lifetime. The IRF, determined by cross correlating the gate and pump pulses, is shorter than the emission time-trace. A convolution of the IRF and the predicted temporal response for a 30 fs decay is also shorter than the measured lifetime. Comparison to the film reveals no change in emission lifetime, while the plasmon enhances the excitation by ~2.6× (based on the increased absorbance at 535 nm) and the emission by ~1.4× (Purcell effect), resulting in a 3–4 times higher emission intensity for the nanoparticles with the same volume of gold, based on the scaling factors in (A). (B) Diagram of interband excitation and emission. A *d*-band electron is excited to an empty level in the *sp*-band near the Fermi energy (purple arrow). An *sp*-band electron radiatively recombines with the *d*-band hole. (C) Diagram of interband excitation followed by Auger scattering. An *sp*-band electron nonradiatively recombines with the *d*-band

hole transferring energy and momentum to another *sp*-band electron that is excited to an empty level above the Fermi energy.

We also compare the time-resolved emission from the gold nanoparticles to the 10 nm gold film overcoated with 30 nm Al_2O_3 (Figure 3A). Importantly, because the nanoparticles are formed from a 10 nm film, the volume of gold that is photoexcited remains the same between the gold nanoparticle sample and the continuous gold film sample under our 2.6 μm beam waist. The emission intensity from the gold nanoparticles at 650±25 nm is 3–4 times greater than the continuous gold film (Figure 3A). When we lower the pump power used on the gold nanoparticles by a factor of three, the emission intensity equally reduces, but the lifetime does not change. For these large, unstructured or 'flawed' gold nanoparticles, plasmon enhancement is overall weak because of a low resonator quality factor. However, our sample design allows for a quantitative comparison to bulk gold, while ensuring the absence of emissive impurities. Furthermore, based on our results we do not expect the d-band hole lifetime to change significantly even for higher quality plasmonic nanostructures.

Finally, we find that the emission lifetime is longer at a redshifted emission wavelength of 730±25 nm (Figure 4A). We assign this emission energy dependence to hot holes cooling to the top of the d-band, assuming both the radiative rate and Auger scattering rate are energy independent.[56] While we do not expect the d-band hole lifetime to follow a Fermi liquid theory dependence over the entire energy range spanning interband and intraband excitations, it may follow a modified Fermi liquid dependence for the holes localized within the 5d-band. Therefore, based on the emission lifetime measured at 650±25 nm, we obtain a Fermi liquid theory dependence of $\tau_h = 210 \pm 20\ fs \cdot eV^2\ (E_i - E_F)^{-2}$, where $E_i - E_F$ is the interband emission energy (1.9±0.08 eV). This relationship predicts a hole lifetime of 72±14 fs for an emission energy of 1.7±0.05 eV (730±25 nm), very close to the measured value of 80±12 fs (Figure 4B). This dependence is further corroborated when considering the results of Varnavski *et al*.,[57] where an instrument limited lifetime of ≤50 fs was measured for colloidally synthesized gold nanospheres in solution at an emission wavelength of 580 nm (2.14 eV). Extrapolating our results to 580 nm yields 46±3 fs, in excellent agreement with Ref. [57]. Thus, we observe the cooling dynamics of hot *d*-band holes to the *d*-band edge through the emission lifetime, as summarized in Figure 4B and depicted in Figure 4C.

We note here that we are ignoring radiative recombination within the *sp*-band following Auger scattering and leading to intraband photoluminescence.[46,47,58,59] While such an emission mechanism is possible, interband recombination is still expected to dominate given the high density of states in the *d*-band and flat density of states for *sp*-band electrons around the Fermi energy.[60] Furthermore, the large nanoparticles studied here have comparatively small Purcell factors, unlike single nanorods with widths below 40 nm,[54] and hence pronounced intraband photoluminescence especially at an excitation wavelength of 535 nm is not expected.

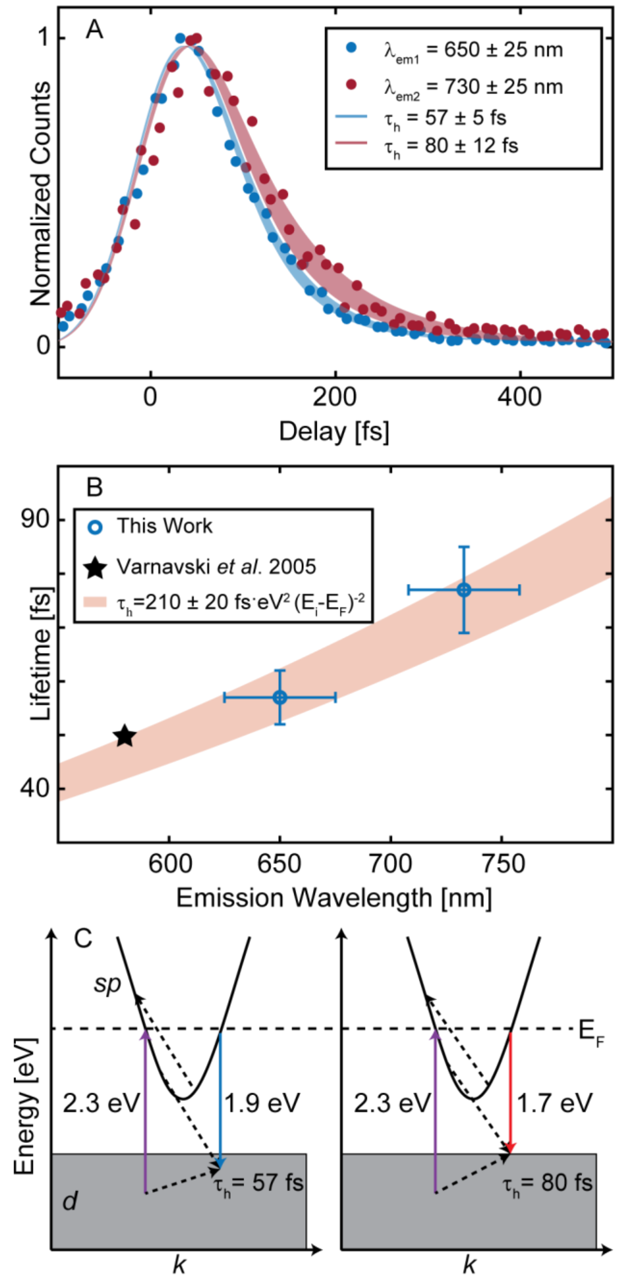

Figure 4. Emission energy dependence of gold nanoparticle emission lifetime. (A) Time-resolved emission of the gold nanoparticles at center emission wavelengths of 650±25 nm (blue) and 730±25 nm (red). The blue and red shaded areas are the 95% confidence intervals for the corresponding decay times from a convolution fit of the IRF with an instantaneous rise and two-phase exponential decay. (B) Energy dependence of the *d*-band hole lifetimes as measured in (A) and from Ref. [57], indicated by blue circles and a black star, respectively. Error bars in x and y are from the upconversion bandwidth and 95% confidence

interval for the convolution fit, respectively. The orange shaded region is the 95% confidence interval predicted by a Fermi liquid theory dependence based off the measured emission lifetime at 650±25 nm. (C) Energy diagram depicting the energy dependent hole scattering as measured by the photoluminescence lifetime.

We directly measured the *d*-band hole lifetime and cooling in plasmonic gold nanoparticles using time-resolved emission upconversion microscopy. This technique is uniquely suited for studying the interband excited *d*-band hot holes, as compared to transient pump-probe spectroscopy that probes the collective relaxation of many excited electrons through electron-electron and electron-phonon scattering, through the dynamic changes in the metal's dielectric function.[30,31,61] In our system, the plasmon enhances the emission intensity from the gold nanoparticles compared to a gold film of the same volume, but we observe no appreciable difference in lifetime. We also observe an emission wavelength dependence for the lifetime, and attribute it to the energy dependent cooling of the hot holes to the *d*-band edge. The main nonradiative relaxation channel for *d*-band holes is Auger scattering, limiting their lifetime to 30–100 fs, similar to the findings from photoemission spectroscopy[35,36,38] and earlier theory on hot hole lifetimes,[29,37,40] while in contrast to more recent theories that appear to overestimate hole-phonon scattering.[21,22] Our results imply that plasmonic photo-oxidation reactions with *d*-band holes must therefore compete on this timescale, explaining the non-negligible yet reportedly low yields.[62]

ASSOCIATED CONTENT

Supporting Information.

The following files are available free of charge. Materials and methods and supplemental figures including beam waist measurement, sample photostability, and pump and gate spectra. (PDF)

AUTHOR INFORMATION

Corresponding Author

Stephan Link - *Department of Chemistry, Center for Adapting Flaws into Features, Department of Electrical and Computer Engineering, Smalley-Curl Institute, Rice University, 6100 Main Street, Houston, Texas 77005, United States*, http://orcid.org/0000-0002-4781-930X; Email: slink@rice.edu

Authors

Stephen A. Lee - *Department of Chemistry, Center for Adapting Flaws into Features, Rice University, 6100 Main Street, Houston, Texas 77005, United States*; http://orcid.org/0000-0003-2614-286X

Christopher T. Kuhs - *U.S. Army DEVCOM Army Research Laboratory-South, 6100 Main Street, Houston, Texas 77005, United States*; http://orcid.org/0000-0002-3168-1836

Emily K. Searles - *Department of Chemistry, Center for Adapting Flaws into Features, Rice University, 6100 Main Street, Houston, Texas 77005, United States*; https://orcid.org/0000-0001-8621-0110

Henry O. Everitt - *U.S. Army DEVCOM Army Research Laboratory-South, Department of Electrical and Computer Engineering, Rice University, 6100 Main Street, Houston, Texas 77005, United States*; https://orcid.org/0000-0002-8141-3768

Christy F. Landes - *Department of Chemistry, Center for Adapting Flaws into Features, Department of Electrical and Computer Engineering, Smalley-Curl Institute, Department of Chemical and Biomolecular Engineering, Rice University, 6100 Main Street, Houston, Texas 77005, United States*; http://orcid.org/0000-0003-4163-6497

Author Contributions

The manuscript was written through contributions of all authors. All authors have given approval to the final version of the manuscript. ‡These authors contributed equally.

Funding Sources

This work was funded by the National Science Foundation, Center for Adapting Flaws into Features (NSF CHE-2124983). SL thanks the Robert A. Welch Foundation for support through the Charles W. Duncan, Jr.-Welch Chair in Chemistry (C-0002). CFL acknowledges funding from the Robert A. Welch Foundation (C-1787) and support through the Kenneth S. Pitzer-Schlumberger Chair in Chemistry. This work was conducted in part using resources of the Shared Equipment Authority at Rice University.

Notes

The authors declare no competing financial interests.

ABBREVIATIONS

Full width at half maximum (FWHM)

Off-axis parabolic (OAP)

Lithium triborate (LBO)

Beta-barium borate (BBO)

Second harmonic generation (SHG)

Third harmonic generation (THG)

Quantum yield (QY)

TOC Figure

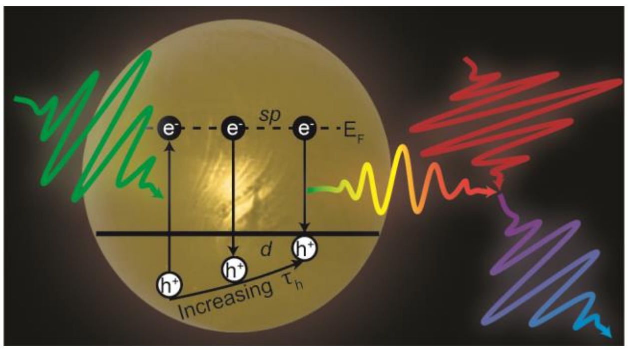

REFERENCES

(1) Brongersma, M. L.; Halas, N. J.; Nordlander, P. Plasmon-Induced Hot Carrier Science and Technology. *Nat. Nanotechnol.* **2015**, *10* (1), 25–34. https://doi.org/10.1038/nnano.2014.311.
(2) Sundararaman, R.; Narang, P.; Jermyn, A. S.; Goddard III, W. A.; Atwater, H. A. Theoretical Predictions for Hot-Carrier Generation from Surface Plasmon Decay. *Nat. Commun.* **2014**, *5* (1), 5788. https://doi.org/10.1038/ncomms6788.
(3) Hartland, G. V.; Besteiro, L. V.; Johns, P.; Govorov, A. O. What's so Hot about Electrons in Metal Nanoparticles? *ACS Energy Lett.* **2017**, *2* (7), 1641–1653. https://doi.org/10.1021/acsenergylett.7b00333.
(4) Furube, A.; Du, L.; Hara, K.; Katoh, R.; Tachiya, M. Ultrafast Plasmon-Induced Electron Transfer from Gold Nanodots into TiO2 Nanoparticles. *J. Am. Chem. Soc.* **2007**, *129* (48), 14852–14853. https://doi.org/10.1021/ja076134v.
(5) Tian, Y.; Tatsuma, T. Mechanisms and Applications of Plasmon-Induced Charge Separation at TiO2 Films Loaded with Gold Nanoparticles. *J. Am. Chem. Soc.* **2005**, *127* (20), 7632–7637. https://doi.org/10.1021/ja042192u.
(6) Voisin, C.; Del Fatti, N.; Christofilos, D.; Vallée, F. Ultrafast Electron Dynamics and Optical Nonlinearities in Metal Nanoparticles. *J. Phys. Chem. B* **2001**, *105* (12), 2264–2280. https://doi.org/10.1021/jp0038153.
(7) Saha, K.; Agasti, S. S.; Kim, C.; Li, X.; Rotello, V. M. Gold Nanoparticles in Chemical and Biological Sensing. *Chem. Rev.* **2012**, *112* (5), 2739–2779. https://doi.org/10.1021/cr2001178.
(8) Nie, S.; Emory, S. R. Probing Single Molecules and Single Nanoparticles by Surface-Enhanced Raman Scattering. *Science* **1997**, *275* (5303), 1102–1106. https://doi.org/10.1126/science.275.5303.1102.
(9) Elghanian, R.; Storhoff, J. J.; Mucic, R. C.; Letsinger, R. L.; Mirkin, C. A. Selective Colorimetric Detection of Polynucleotides Based on the Distance-Dependent Optical Properties of Gold Nanoparticles. *Science* **1997**, *277* (5329), 1078–1081. https://doi.org/10.1126/science.277.5329.1078.
(10) Carron, K. T.; Fluhr, W.; Meier, M.; Wokaun, A.; Lehmann, H. W. Resonances of Two-Dimensional Particle Gratings in Surface-Enhanced Raman Scattering. *J. Opt. Soc. Am. B* **1986**, *3* (3), 430–440. https://doi.org/10.1364/JOSAB.3.000430.
(11) Rodriguez, S. R. K.; Schaafsma, M. C.; Berrier, A.; Gómez Rivas, J. Collective Resonances in Plasmonic Crystals: Size Matters. *Phys. B Condens. Matter* **2012**, *407* (20), 4081–4085. https://doi.org/10.1016/j.physb.2012.03.053.
(12) Deng, S.; Li, R.; Park, J.-E.; Guan, J.; Choo, P.; Hu, J.; Smeets, P. J. M.; Odom, T. W. Ultranarrow Plasmon Resonances from Annealed Nanoparticle Lattices. *Proc. Natl. Acad. Sci.* **2020**, *117* (38), 23380–23384. https://doi.org/10.1073/pnas.2008818117.
(13) Knight, M. W.; Sobhani, H.; Nordlander, P.; Halas, N. J. Photodetection with Active Optical Antennas. *Science* **2011**, *332* (6030), 702–704. https://doi.org/10.1126/science.1203056.
(14) Wu, K.; Chen, J.; McBride, J. R.; Lian, T. Efficient Hot-Electron Transfer by a Plasmon-Induced Interfacial Charge-Transfer Transition. *Science* **2015**, *349* (6248), 632–635. https://doi.org/10.1126/science.aac5443.

(15) Zhang, Y.; He, S.; Guo, W.; Hu, Y.; Huang, J.; Mulcahy, J. R.; Wei, W. D. Surface-Plasmon-Driven Hot Electron Photochemistry. *Chem. Rev.* **2018**, *118* (6), 2927–2954. https://doi.org/10.1021/acs.chemrev.7b00430.
(16) Kim, Y.; Smith, J. G.; Jain, P. K. Harvesting Multiple Electron–Hole Pairs Generated through Plasmonic Excitation of Au Nanoparticles. *Nat. Chem.* **2018**, *10* (7), 763–769. https://doi.org/10.1038/s41557-018-0054-3.
(17) Moskovits, M. The Case for Plasmon-Derived Hot Carrier Devices. *Nat. Nanotechnol.* **2015**, *10* (1), 6–8. https://doi.org/10.1038/nnano.2014.280.
(18) Harutyunyan, H.; Suchanek, F.; Lemasters, R.; Foley, J. J. Hot-Carrier Dynamics in Catalysis. *MRS Bull.* **2020**, *45* (1), 32–36. https://doi.org/10.1557/mrs.2019.291.
(19) Jeffries, W. R.; Park, K.; Vaia, R. A.; Knappenberger, K. L. Jr. Resolving Electron–Electron Scattering in Plasmonic Nanorod Ensembles Using Two-Dimensional Electronic Spectroscopy. *Nano Lett.* **2020**, *20* (10), 7722–7727. https://doi.org/10.1021/acs.nanolett.0c03272.
(20) Jollans, T.; Caldarola, M.; Sivan, Y.; Orrit, M. Effective Electron Temperature Measurement Using Time-Resolved Anti-Stokes Photoluminescence. *J. Phys. Chem. A* **2020**, *124* (34), 6968–6976. https://doi.org/10.1021/acs.jpca.0c06671.
(21) Bernardi, M.; Mustafa, J.; Neaton, J. B.; Louie, S. G. Theory and Computation of Hot Carriers Generated by Surface Plasmon Polaritons in Noble Metals. *Nat. Commun.* **2015**, *6* (1), 7044. https://doi.org/10.1038/ncomms8044.
(22) Brown, A. M.; Sundararaman, R.; Narang, P.; Goddard, W. A. I.; Atwater, H. A. Nonradiative Plasmon Decay and Hot Carrier Dynamics: Effects of Phonons, Surfaces, and Geometry. *ACS Nano* **2016**, *10* (1), 957–966. https://doi.org/10.1021/acsnano.5b06199.
(23) Jin, H.; Kahk, J. M.; Papaconstantopoulos, D. A.; Ferreira, A.; Lischner, J. Plasmon-Induced Hot Carriers from Interband and Intraband Transitions in Large Noble Metal Nanoparticles. *PRX Energy* **2022**, *1* (1), 013006. https://doi.org/10.1103/PRXEnergy.1.013006.
(24) Zhang, Y.; Guo, W.; Zhang, Y.; Wei, W. D. Plasmonic Photoelectrochemistry: In View of Hot Carriers. *Adv. Mater.* **2021**, *33* (46), 2006654. https://doi.org/10.1002/adma.202006654.
(25) Dunklin, J. R.; Rose, A. H.; Zhang, H.; Miller, E. M.; van de Lagemaat, J. Plasmonic Hot Hole Transfer in Gold Nanoparticle-Decorated Transition Metal Dichalcogenide Nanosheets. *ACS Photonics* **2020**, *7* (1), 197–202. https://doi.org/10.1021/acsphotonics.9b01393.
(26) Al-Zubeidi, A.; Hoener, B. S.; Collins, S. S. E.; Wang, W.; Kirchner, S. R.; Hosseini Jebeli, S. A.; Joplin, A.; Chang, W.-S.; Link, S.; Landes, C. F. Hot Holes Assist Plasmonic Nanoelectrode Dissolution. *Nano Lett.* **2019**, *19* (2), 1301–1306. https://doi.org/10.1021/acs.nanolett.8b04894.
(27) Schlather, A. E.; Manjavacas, A.; Lauchner, A.; Marangoni, V. S.; DeSantis, C. J.; Nordlander, P.; Halas, N. J. Hot Hole Photoelectrochemistry on Au@SiO_2@Au Nanoparticles. *J. Phys. Chem. Lett.* **2017**, *8* (9), 2060–2067. https://doi.org/10.1021/acs.jpclett.7b00563.
(28) DuChene, J. S.; Tagliabue, G.; Welch, A. J.; Cheng, W.-H.; Atwater, H. A. Hot Hole Collection and Photoelectrochemical CO2 Reduction with Plasmonic Au/p-GaN Photocathodes. *Nano Lett.* **2018**, *18* (4), 2545–2550. https://doi.org/10.1021/acs.nanolett.8b00241.
(29) Zhukov, V. P.; Chulkov, E. V.; Echenique, P. M. Lifetimes of d Holes in Cu and Au: Full-Potential LMTO Approach. *Phys. Rev. B* **2003**, *68* (4), 045102. https://doi.org/10.1103/PhysRevB.68.045102.

(30) Hartland, G. V. Optical Studies of Dynamics in Noble Metal Nanostructures. *Chem. Rev.* **2011**, *111* (6), 3858–3887. https://doi.org/10.1021/cr1002547.
(31) Harutyunyan, H.; Martinson, A. B. F.; Rosenmann, D.; Khorashad, L. K.; Besteiro, L. V.; Govorov, A. O.; Wiederrecht, G. P. Anomalous Ultrafast Dynamics of Hot Plasmonic Electrons in Nanostructures with Hot Spots. *Nat. Nanotechnol.* **2015**, *10* (9), 770–774. https://doi.org/10.1038/nnano.2015.165.
(32) Bauer, M.; Marienfeld, A.; Aeschlimann, M. Hot Electron Lifetimes in Metals Probed by Time-Resolved Two-Photon Photoemission. *Prog. Surf. Sci.* **2015**, *90* (3), 319–376. https://doi.org/10.1016/j.progsurf.2015.05.001.
(33) Cao, J.; Gao, Y.; Elsayed-Ali, H. E.; Miller, R. J. D.; Mantell, D. A. Femtosecond Photoemission Study of Ultrafast Electron Dynamics in Single-Crystal Au(111) Films. *Phys. Rev. B* **1998**, *58* (16), 10948–10952. https://doi.org/10.1103/PhysRevB.58.10948.
(34) Petek, H.; Ogawa, S. Femtosecond Time-Resolved Two-Photon Photoemission Studies of Electron Dynamics in Metals. *Prog. Surf. Sci.* **1997**, *56* (4), 239–310. https://doi.org/10.1016/S0079-6816(98)00002-1.
(35) Knoesel, E.; Hotzel, A.; Wolf, M. Ultrafast Dynamics of Hot Electrons and Holes in Copper: Excitation, Energy Relaxation, and Transport Effects. *Phys. Rev. B* **1998**, *57* (20), 12812–12824. https://doi.org/10.1103/PhysRevB.57.12812.
(36) Matzdorf, R.; Gerlach, A.; Theilmann, F.; Meister, G.; Goldmann, A. New Lifetime Estimates for D-Band Holes at Noble Metal Surfaces. *Appl. Phys. B* **1999**, *68* (3), 393–395. https://doi.org/10.1007/s003400050637.
(37) Gerlach, A.; Berge, K.; Goldmann, A.; Campillo, I.; Rubio, A.; Pitarke, J. M.; Echenique, P. M. Lifetime of d Holes at Cu Surfaces: Theory and Experiment. *Phys. Rev. B* **2001**, *64* (8), 085423. https://doi.org/10.1103/PhysRevB.64.085423.
(38) Petek, H.; Nagano, H.; Ogawa, S. Hole Decoherence of d Bands in Copper. *Phys. Rev. Lett.* **1999**, *83* (4), 832–835. https://doi.org/10.1103/PhysRevLett.83.832.
(39) Quinn, J. J. Range of Excited Electrons in Metals. *Phys. Rev.* **1962**, *126* (4), 1453–1457. https://doi.org/10.1103/PhysRev.126.1453.
(40) Campillo, I.; Rubio, A.; Pitarke, J. M.; Goldmann, A.; Echenique, P. M. Hole Dynamics in Noble Metals. *Phys. Rev. Lett.* **2000**, *85* (15), 3241–3244. https://doi.org/10.1103/PhysRevLett.85.3241.
(41) Mooradian, A. Photoluminescence of Metals. *Phys. Rev. Lett.* **1969**, *22* (5), 185–187. https://doi.org/10.1103/PhysRevLett.22.185.
(42) Boyd, G. T.; Yu, Z. H.; Shen, Y. R. Photoinduced Luminescence from the Noble Metals and Its Enhancement on Roughened Surfaces. *Phys. Rev. B* **1986**, *33* (12), 7923–7936. https://doi.org/10.1103/PhysRevB.33.7923.
(43) Baraldi, G.; Carrada, M.; Toudert, J.; Ferrer, F. J.; Arbouet, A.; Paillard, V.; Gonzalo, J. Preventing the Degradation of Ag Nanoparticles Using an Ultrathin A-Al2O3 Layer as Protective Barrier. *J. Phys. Chem. C* **2013**, *117* (18), 9431–9439. https://doi.org/10.1021/jp401421m.
(44) Foerster, B.; Joplin, A.; Kaefer, K.; Celiksoy, S.; Link, S.; Sönnichsen, C. Chemical Interface Damping Depends on Electrons Reaching the Surface. *ACS Nano* **2017**, *11* (3), 2886–2893. https://doi.org/10.1021/acsnano.6b08010.
(45) Sönnichsen, C.; Franzl, T.; Wilk, T.; von Plessen, G.; Feldmann, J.; Wilson, O.; Mulvaney, P. Drastic Reduction of Plasmon Damping in Gold Nanorods. *Phys. Rev. Lett.* **2002**, *88* (7), 077402. https://doi.org/10.1103/PhysRevLett.88.077402.

(46) Yorulmaz, M.; Khatua, S.; Zijlstra, P.; Gaiduk, A.; Orrit, M. Luminescence Quantum Yield of Single Gold Nanorods. *Nano Lett.* **2012**, *12* (8), 4385–4391. https://doi.org/10.1021/nl302196a.
(47) Dulkeith, E.; Niedereichholz, T.; Klar, T. A.; Feldmann, J.; von Plessen, G.; Gittins, D. I.; Mayya, K. S.; Caruso, F. Plasmon Emission in Photoexcited Gold Nanoparticles. *Phys. Rev. B* **2004**, *70* (20), 205424. https://doi.org/10.1103/PhysRevB.70.205424.
(48) Fang, Y.; Chang, W.-S.; Willingham, B.; Swanglap, P.; Dominguez-Medina, S.; Link, S. Plasmon Emission Quantum Yield of Single Gold Nanorods as a Function of Aspect Ratio. *ACS Nano* **2012**, *6* (8), 7177–7184. https://doi.org/10.1021/nn3022469.
(49) Haug, T.; Klemm, P.; Bange, S.; Lupton, J. M. Hot-Electron Intraband Luminescence from Single Hot Spots in Noble-Metal Nanoparticle Films. *Phys. Rev. Lett.* **2015**, *115* (6), 067403. https://doi.org/10.1103/PhysRevLett.115.067403.
(50) Roloff, L.; Klemm, P.; Gronwald, I.; Huber, R.; Lupton, J. M.; Bange, S. Light Emission from Gold Nanoparticles under Ultrafast Near-Infrared Excitation: Thermal Radiation, Inelastic Light Scattering, or Multiphoton Luminescence? *Nano Lett.* **2017**, *17* (12), 7914–7919. https://doi.org/10.1021/acs.nanolett.7b04266.
(51) Huang, J.; Wang, W.; Murphy, C. J.; Cahill, D. G. Resonant Secondary Light Emission from Plasmonic Au Nanostructures at High Electron Temperatures Created by Pulsed-Laser Excitation. *Proc. Natl. Acad. Sci.* **2014**, *111* (3), 906–911. https://doi.org/10.1073/pnas.1311477111.
(52) Khriachtchev, L.; Heikkilä, L.; Kuusela, T. Red Photoluminescence of Gold Island Films. *Appl. Phys. Lett.* **2001**, *78* (14), 1994–1996. https://doi.org/10.1063/1.1359491.
(53) Lemasters, R.; Zhang, C.; Manjare, M.; Zhu, W.; Song, J.; Urazhdin, S.; Lezec, H. J.; Agrawal, A.; Harutyunyan, H. Ultrathin Wetting Layer-Free Plasmonic Gold Films. *ACS Photonics* **2019**, *6* (11), 2600–2606. https://doi.org/10.1021/acsphotonics.9b00907.
(54) Ostovar, B.; Cai, Y.-Y.; Tauzin, L. J.; Lee, S. A.; Ahmadivand, A.; Zhang, R.; Nordlander, P.; Link, S. Increased Intraband Transitions in Smaller Gold Nanorods Enhance Light Emission. *ACS Nano* **2020**, *14* (11), 15757–15765. https://doi.org/10.1021/acsnano.0c06771.
(55) Apell, P.; Monreal, R.; Lundqvist, S. Photoluminescence of Noble Metals. *Phys. Scr.* **1988**, *38* (2), 174–179. https://doi.org/10.1088/0031-8949/38/2/012.
(56) Strickler, S. J.; Berg, R. A. Relationship between Absorption Intensity and Fluorescence Lifetime of Molecules. *J. Chem. Phys.* **1962**, *37* (4), 814–822. https://doi.org/10.1063/1.1733166.
(57) Varnavski, O. P.; Goodson, T.; Mohamed, M. B.; El-Sayed, M. A. Femtosecond Excitation Dynamics in Gold Nanospheres and Nanorods. *Phys. Rev. B* **2005**, *72* (23), 235405. https://doi.org/10.1103/PhysRevB.72.235405.
(58) Cai, Y.-Y.; Tauzin, L. J.; Ostovar, B.; Lee, S.; Link, S. Light Emission from Plasmonic Nanostructures. *J. Chem. Phys.* **2021**, *155* (6), 060901. https://doi.org/10.1063/5.0053320.
(59) Cheng, Y.; Lu, G.; He, Y.; Shen, H.; Zhao, J.; Xia, K.; Gong, Q. Luminescence Quantum Yields of Gold Nanoparticles Varying with Excitation Wavelengths. *Nanoscale* **2016**, *8* (4), 2188–2194. https://doi.org/10.1039/C5NR07343J.
(60) Ramchandani, M. G. Energy Band Structure of Gold. *J. Phys. C Solid State Phys.* **1970**, *3* (1S), S1. https://doi.org/10.1088/0022-3719/3/1S/301.
(61) Sun, C.-K.; Vallée, F.; Acioli, L. H.; Ippen, E. P.; Fujimoto, J. G. Femtosecond-Tunable Measurement of Electron Thermalization in Gold. *Phys. Rev. B* **1994**, *50* (20), 15337–15348. https://doi.org/10.1103/PhysRevB.50.15337.

(62) Yu, S.; Jain, P. K. The Chemical Potential of Plasmonic Excitations. *Angew. Chem. Int. Ed.* **2020**, *59* (5), 2085–2088. https://doi.org/10.1002/anie.201914118.